

# Assessment of Uncertainty in ROLO Lunar Irradiance for On-orbit Calibration

Thomas C. Stone<sup>a</sup> and Hugh H. Kieffer<sup>b</sup>

<sup>a</sup> US Geological Survey, 2255 N. Gemini Drive, Flagstaff, AZ, 86001

<sup>b</sup> Celestial Reasonings, 2256 Christmas Tree Lane, Carson City, NV 89703

## ABSTRACT

A system to provide radiometric calibration of remote sensing imaging instruments on-orbit using the Moon has been developed by the US Geological Survey Robotic Lunar Observatory (ROLO) project. ROLO has developed a model for lunar irradiance which treats the primary geometric variables of phase and libration explicitly. The model fits hundreds of data points in each of 23 VNIR and 9 SWIR bands; input data are derived from lunar radiance images acquired by the project's on-site telescopes, calibrated to exoatmospheric radiance and converted to disk-equivalent reflectance. Experimental uncertainties are tracked through all stages of the data processing and modeling. Model fit residuals are  $\sim 1\%$  in each band over the full range of observed phase and libration angles. Application of ROLO lunar calibration to SeaWiFS has demonstrated the capability for long-term instrument response trending with precision approaching 0.1% per year. Current work involves assessing the error in absolute responsivity and relative spectral response of the ROLO imaging systems, and propagation of error through the data reduction and modeling software systems with the goal of reducing the uncertainty in the absolute scale, now estimated at 5–10%. This level is similar to the scatter seen in ROLO lunar irradiance comparisons of multiple spacecraft instruments that have viewed the Moon. A field calibration campaign involving NASA and NIST has been initiated that ties the ROLO lunar measurements to the NIST (SI) radiometric scale.

**Keywords:** On-orbit calibration, Moon, Irradiance, Uncertainty

## 1. INTRODUCTION

Production of reliable climate data records from satellite imaging instruments requires determination of the long-term stability of sensor performance on-orbit. The USGS Robotic Lunar Observatory (ROLO) program has developed the capability for using the Moon as a spectral reference source for on-orbit calibration.<sup>12</sup> The advantages and complications of using the Moon as a calibration target have been discussed previously.<sup>3,4,10</sup>

Lunar calibrations conducted to date by ROLO have involved comparing spacecraft observations of the Moon against a model for lunar disk-equivalent irradiance.<sup>11,20</sup> The model generates the lunar irradiance at the spacecraft instrument wavelengths for the precise time and location of observation, determined from an empirical function for lunar reflectance that accounts for the variation in lunar brightness with phase and libration. This capability derives from a 6+ year archive of lunar radiance images acquired by the ROLO ground-based observational program. At-telescope images of the Moon are corrected to exoatmospheric using nightly extinction measurements of stars and calibrated to radiance, then spatially integrated to disk-equivalent irradiance and converted to reflectance using the effective solar spectral irradiance computed for the ROLO instrument bands. The model fits hundreds of data points in each band covering a wide range of phase and libration angles; its analytic form (see §3) was designed by detailed analysis of the fit residuals.

Monitoring a spacecraft instrument response over time using repeated observations of the Moon requires only that the lunar model correctly predict variations in the lunar photometric behavior for the particular geometries of the spacecraft observations. This has been demonstrated for SeaWiFS. The SeaWiFS team has developed a long-term correction for ocean-leaving radiances with a relative precision on the order of 0.1% per year.<sup>2</sup>

---

Further author information: (Send correspondence to T.C.S.)

e-mail: [tstone@usgs.gov](mailto:tstone@usgs.gov), telephone: 928-556-7381

H.H.K.: e-mail: [hkieffer@charter.net](mailto:hkieffer@charter.net)

However, intercomparison of different instruments that have viewed the Moon is more specifically dependent upon accuracy in the absolute scale and the spectral shape of the model-derived irradiance.<sup>11</sup>

Absolute calibration of the ROLO systems has proceeded along several pathways; the current absolute scale for ROLO irradiance data is derived from observations of the star Vega. The model-generated lunar reflectance displays some irregular spectral structure that is not attributable to properties of the Moon, requiring a correction derived from laboratory measurements of returned Apollo samples.<sup>11,20</sup> Estimated uncertainty in the ROLO model absolute scale is currently 5–10%, which is comparable to the scatter seen in spacecraft calibration comparisons,<sup>11</sup> but in excess of project goals.<sup>12</sup>

A current major focus of the ROLO project is the evaluation of experimental uncertainties in the ROLO observational data stream and the traceability to NIST (SI) radiometric standards. One goal is to remove the current dependence upon a stellar source (and hence on an atmospheric extinction correction) for the definition of the system absolute response. This paper describes several elements of ROLO lunar calibration in the context of accounting for sources of uncertainty, providing quantitative evaluations where these have been derived.

## 2. LUNAR IMAGES AND IRRADIANCE DATA

The ROLO radiometric characterization of the Moon is founded upon a multi-year database of lunar radiance images acquired by the project’s ground-based telescopes. Routine ROLO observations span lunar phases from near-eclipse to First and Last Quarter. The Moon and stars are imaged in 23 VNIR bands onto a 512-pixel square CCD (Moon diameter  $\sim 500$  pixels), and 9 SWIR bands with a 256-pixel square HgCdTe photoconductive array (dia.  $\sim 250$  pixels). Celestial target selection, camera control, and image data recording are virtually fully automated.<sup>1</sup> The ROLO database now contains over 85 000 individual lunar images and several hundred thousand stellar images.

Data for the irradiance model inputs are derived from telescope images, corrected for detector artifacts<sup>21</sup> and normalized to 1-second exposure. Lunar image pixels (DN/sec) are integrated over the entire disk, regardless of the illuminated fraction, to give an effective irradiance, which follows the “one-over-R-squared” law with respect to Moon-observer distance. The irradiance sums are converted to exoatmospheric quantities  $\mathcal{I}$  in radiometric units:

$$\mathcal{I} = (I_{\Sigma} \cdot C_L \cdot C_{ext}) \cdot \Omega_p \cdot f_D \quad (1)$$

where  $I_{\Sigma}$  is the image disk-integrated irradiance and  $\Omega_p$  is the solid angle of a pixel; the radiance calibration  $C_L$  and atmospheric extinction correction  $C_{ext}$  are discussed in more detail below. Observational data are corrected to the standard distances adopted by ROLO:

$$f_D = \left( \frac{\text{Moon-observer distance (km)}}{384400} \right)^2 \cdot (\text{Moon-Sun distance (AU)})^2 \quad (2)$$

Table 1 lists sources of error tracked during ROLO lunar image processing. At all stages of the data reduction, uncertainties are evaluated using statistical methods; sample values for one randomly selected VNIR image are given in the table. Also listed are “practical estimates”, which reflect offline evaluations of errors observed in the derived quantities. Normally the discrete statistical uncertainties in the upper part of the table are propagated through the processing steps using standard error combination practices to give a cumulative pixel error value for each band. Uncertainties in derived quantities such as disk centering and irradiance integration utilize the pixel error in formal error propagation computations appropriate for the operations.

### 2.1. Detector Artifact Correction

For the detector correction operations (bias, dark current and flatfielding) uncertainties are derived from statistical sampling of pixels. The ROLO VNIR CCD has two special readout regions that are unconnected to imaging pixels, from which the bias level is measured and its associated error evaluated. Dark images are acquired in dedicated sessions at the beginning and end of each observing night for a series of exposure times. A function for the dark current is fitted for each pixel, linear for the VNIR instrument. A dark correction “image” is constructed

**Table 1.** Uncertainties tracked during ROLO image processing, typical average values for VNIR

Processing Step	Relative Uncertainty (%)	
	Statistics-based	Practical Estimates
bias correction	0.0368	
dark current correction	0.0846	
image flatfielding	$2.23 \times 10^{-4}$	
lunar disk centering	0.0750	0.4 ( $\sim 1$ pixel)
sum to irradiance	0.00432	0.2
atmospheric correction*	0.743	0.69
radiance calibration*	0.216	3.1

\*exclusive of absolute scale

from the fit parameters, which includes statistical errors derived from the fitting process. Uncertainties in the dark correction are generated for each corrected image (band) as an average over all pixels.

Evaluation of dark current for the SWIR detector is more complicated. In addition to the twice-nightly dedicated dark acquisitions, a dark frame is taken with each 9-filter sequence, viewing a brass plug installed in one filter hole, held at liquid nitrogen temperature. The entire ensemble of dark frames acquired over the night is fitted by a time-dependent polynomial for the dark current for each pixel. The bias level is defined as the zero exposure time point, also a time-dependent quantity. Uncertainties for both dark and bias corrections are derived from the fit residuals; typical values for SWIR images are  $\sim 0.3\%$ .

Flatfielding images for both instruments are generated from observations of a diffuse reflective panel illuminated by a 1000-Watt quartz-tungsten-halogen lamp. The ROLO standard processing routines for removing detector artifacts generate a pixel error value; the cumulative error over all pixels in a flatfielding image defines the flatfield correction uncertainty for each band.

Integration to irradiance requires accurate location of the Moon in the ROLO processed images. The current software version finds the lunar disk center by fitting a circular arc to  $160^\circ$  of the bright limb, defined as the inflection point of the transition from lunar surface to sky background. The limb radius is computed at  $1.35 \times$  (radius in pixels) locations along the arc, and the center point is adjusted based on the radius deviations. This process is iterated until the change in the center point location is less than  $10^{-4}$  pixel in sample and line. The disk centering error is determined from the standard deviation of the final limb radius measurements. However, offline analysis has shown a spatial jitter in the lunar image co-registration of  $\sim 1$  pixel; we attribute this to an incomplete definition of the bright limb from the disk-to-background transition.

Uncertainty in the irradiance sums is derived from a formal error analysis, starting from the pixel error value. Terms are included to account for the sky background subtraction and a line spread correction for the Moon.

## 2.2. Atmospheric Extinction Correction

Atmospheric corrections for ROLO lunar image data are developed from nightly observations of stars. The majority of telescope observing time,  $\sim 70\%$  when the Moon is viewable (100% otherwise), has been dedicated to stellar observations. Star images are integrated to at-telescope irradiance and input to a model for the transmission of multiple independent atmospheric constituents, treating the individual component absorptions as time-dependent variables that are coupled across all bands. Fitting the nightly stellar data yields a set of parameters describing the absorption strength of each constituent as a function of time. These are used in turn to define the extinction for the acquisition times of the lunar images.

A typical nightly observing session targets  $\sim 12$  different extinction stars, observed 10 to 15 times through the night. The positions of selected stars are spread throughout the sky, generally within  $30^\circ$  of the ecliptic. Standard ROLO procedures limit observations to  $60^\circ$  from zenith, and some stars are not accessible for the entire night; this places a lower limit on the uncertainty achievable from nightly extinction modeling. To better constrain the extinction solution, a table of exoatmospheric stellar irradiances (instrument units) has been developed from a dedicated reprocessing of all ROLO stellar data, during which the extinction computations were iterated

multiple times to converge on best-fit exoatmospheric values for all ROLO standard stars. When these constant exoatmospheric data are used, the extinction model includes a term for nightly variations in instrument gain.

The extinction of starlight by seven atmospheric absorbing components is modeled by a system of linear equations in the stellar irradiances  $I_\star$  (DN) converted to astronomic magnitudes  $m = \frac{-2.5}{\ln(10.0)} \ln(I_\star)$ . For each star observation in band  $k$ :

$$m_{\text{obs},k} = m_{0,k} + \sum_{i=1}^7 (\kappa_{i,k} \rho_{i,k} X) + g_k \quad (3)$$

where  $m_0$  is the exoatmospheric magnitude,  $g$  is the instrument gain term,  $X$  is airmass, and the time-dependent absorption strengths  $\rho_i$  are represented by Chebyshev polynomials for the “density” of each component:

$$\rho = C_0 + C_1 t + C_2 (2t^2 - 1) \quad (4)$$

where the observation time between 00:00 and 15:00 UTC is mapped onto the interval  $t=[-1:1]$  (mean local solar midnight  $\approx 07:30$  UTC at the ROLO location). The absorption coefficients  $\kappa_i$  have been developed from atmospheric transmission spectra generated using MODTRAN version 3.7, specifying a vertical path 2 km to 200 km (appropriate for Flagstaff), the 1976 standard atmosphere, mid-latitude winter conditions. ROLO has developed and implemented a modification of the MODTRAN spectral interpolation routine to smooth cusp-like discontinuities seen in the outputs for aerosols. The atmospheric transmission curves were convolved with the relative spectral response functions for the ROLO bands, weighted by model stellar spectra appropriate for the color-magnitude classifications of the ROLO standard stars.

The system of equations 3 and 4 is solved for all star observations in a night using a least-squares gradient reduction technique. Uncertainties in the observational data are developed from the image pixel errors, and carried with the  $m_{\text{obs}}$  vector. The solution generates uncertainty values for each output parameter  $C_{n,i,k}$ , thus enabling propagation of the uncertainty to the lunar extinction corrections.

The statistical uncertainty in the atmospheric extinction correction represents a lower limit on the actual uncertainty of this correction. Another estimate of this results from the residuals of the model fits (see §3), which are highly overdetermined. The mean absolute fit residual for the VNIR bands is 0.69% and for the SWIR bands is 1.66%. This comparison suggests that the formal statistical assessment of the atmospheric correction is capturing most of the relative error. Possible systematic errors, e.g in the formulation of the absorption coefficients, will influence the absolute accuracy of the extinction correction; neither the statistical interpretation nor the model fit residuals account for this.

### 2.3. Absolute Calibration

Development of a radiometric scale for ROLO lunar data has evolved from the original project concept, which utilized near-field observations of a diffuse reflective panel illuminated by a calibrated 1000-Watt FEL lamp. The stability of the lamp output under the outdoor environmental conditions at ROLO could not meet the project specification for absolute accuracy. The currently used calibration is based upon observations of the star Vega, both by ROLO and in published photometric measurements. Following the method described in Ref. 8, absolute photon flux measurements<sup>9,22</sup> for Vega were used to scale a model stellar spectrum,<sup>5</sup> which was then convolved with the ROLO band spectral response functions to give the absolute flux in each band. In a dedicated re-processing of all ROLO observations that contain Vega, including special high-zenith angle measurements, the extinction correction algorithm was iterated to cull outlier points and converge on exoatmospheric instrument response rates (DN) for Vega. The calibration is derived from the flux/DN-rate ratio, modified by a time-dependent model for long-term degradation of the telescope optics.

The uncertainty in this star-based calibration can be no less than that of the astronomical photometric measurements upon which it is based. A measurement uncertainty of 1.5% is cited for the Vega flux at 555.6 nm, the point used to scale the visible-wavelength absolute energy distribution.<sup>9</sup> The reported experimental error for the IR measurements is  $\sim 4\%$ .<sup>22</sup> The random error introduced by convolving the instrument passbands is estimated to be  $\sim 1\%$  or less.<sup>8</sup> The statistical uncertainty listed in Table 1 is derived from propagating the stellar image integration error through the calibration development described above, and therefore does not

include these absolute flux measurement uncertainties. Further details on the relative calibration uncertainty are given in §3.

The ROLO instrument relative spectral response (RSR) functions are a critical component of the star-based absolute calibration, entering into the computations of both the in-band Vega absolute flux and the extinction calculations used to derive the exoatmospheric instrument response to Vega. RSR curves for the ROLO bands were generated from the manufacturers’ measurements for the filter transmissions, augmented by precision transmission measurements conducted at the University of Arizona Optical Sciences Center for some filters, then convolving the detector quantum efficiency and an empirical reflection spectrum for aluminum.<sup>6</sup> For a Cassegrain configuration such as the ROLO telescopes, the nominal filter passbands are affected by the wavelength shift induced in multilayer interference filters by off-normal incidence. A correction has been developed by ROLO based on the formula for angle shift:

$$\lambda = \lambda_0 \sqrt{1 - \left(\frac{n_o}{n_e}\right)^2 \sin^2 \theta} \quad (5)$$

where  $n_o$  is the external medium refractive index (real part of the complex index of refraction) and  $n_e$  is the effective refractive index of the filter dielectric spacer. The normal-incidence filter bandpasses are convolved with the calculated wavelength shifts, weighted by the solid angle of the ROLO telescope optical feed. The modeled passbands show effective center wavelength shifts of a few nm and some spreading of the spectral shape.

In an effort aimed at reducing uncertainty in the ROLO absolute scale, a field calibration campaign has been initiated involving NASA EOS calibration personnel, the remote sensing group at the University of Arizona, and the radiometry group at NIST. A collimated light source was designed and built by ROLO, comprising an on-axis system that fills the FOV of the ROLO telescopes. An “artificial moon” radiance source sits at the focus of the collimating mirror; the source is small enough that it is masked by the ROLO telescopes’ secondary mirrors. Two QTH lamps, 9-Watt and 2-Watt, provide two radiance levels compatible with the ROLO VNIR and SWIR sensor systems. Calibrations of the source at both levels were conducted at the NIST FASCAL facility. During field campaigns at ROLO, the source radiance is monitored by repeated transfer calibrations to a NIST field-deployable integrating sphere source. Results from these measurements are still preliminary, but have defined the baseline absolute radiometric response for the ROLO instruments.

As part of the field calibration campaign, the ROLO collimator has been utilized to measure the RSR for several bands through the full optical system. Monochromatic light from tunable lasers provided by the NIST Traveling SIRCUS facility was fiber-optic coupled into the collimator source. The source radiance and the ROLO system response were both measured as the lasers were scanned in wavelength over the passbands. Figure 1 plots the spectral response for the ROLO 412 nm band, showing the nominal RSR developed from the normal-incidence filter transmission, quantum efficiency, and aluminum reflectivity (triangles); the modeled off-axis wavelength shift passband (X’s); and the NIST Traveling SIRCUS field measurements (squares). Because the SIRCUS procedure produces a relative measurement, this curve been scaled to the average peak transmission of the other two. The off-axis model appears to overestimate the wavelength shift for this band.

An additional uncertainty affecting the Vega-based calibration, as yet unquantified, concerns the validity of using a stellar (i.e. point) light source to calibrate an extended radiance image such as the lunar disk. Published results providing a quantitative correction have not been found in a literature search. Examination of this effect is planned for the continued field calibration activities at ROLO, using a series of aperture sizes with the collimated light source.

### 3. ROLO LUNAR REFLECTANCE MODEL

Development of an analytic model to fit the ROLO lunar irradiance database has followed an empirical approach. Fitting is done in unitless reflectance, converted from the disk-integrated irradiance  $\mathcal{I}_k$  of equation 1:

$$\mathcal{I}_k = A_k \cdot \Omega_M E_{Sk} / \pi \quad (6)$$

where  $A_k$  is the disk-equivalent reflectance (albedo),  $\Omega_M = 6.436 \times 10^{-5}$  sr is the solid angle of the Moon, and  $E_{Sk}$  is the solar spectral irradiance in band  $k$  at the effective wavelength for solar radiation. The current version

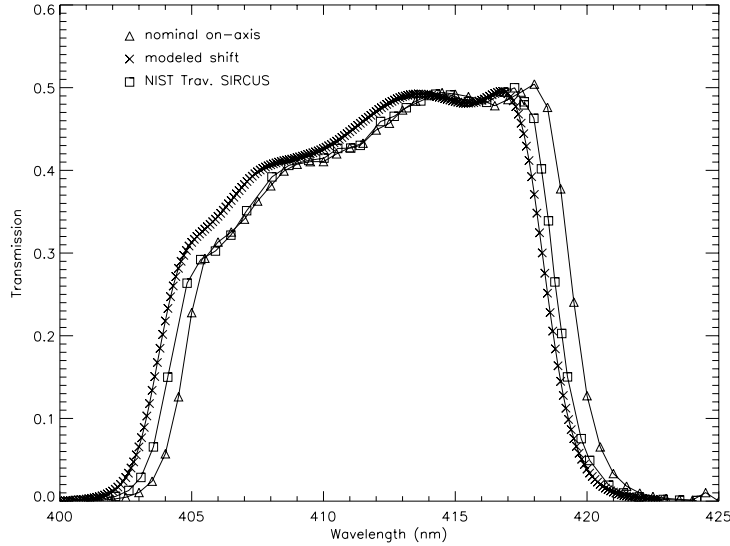


**Figure 1.** Spectral response curves for the ROLO 412 nm band

of the ROLO model gives disk reflectance in terms of the primary geometric variables of phase and libration:

$$\ln A_k = \sum_{i=0}^3 a_{ik} g^i + \sum_{j=1}^3 b_{jk} \Phi^{2j-1} + c_1 \theta + c_2 \phi + c_3 \Phi \theta + c_4 \Phi \phi + d_{1k} e^{-g/p_1} + d_{2k} e^{-g/p_2} + d_{3k} \cos((g - p_3)/p_4) \quad (7)$$

where  $g$  is the absolute phase angle,  $\theta$  and  $\phi$  are the selenographic latitude and longitude of the observer, and  $\Phi$  is the selenographic longitude of the Sun.

The form of equation 7 was developed with the goal of fitting the data to the extent that no correlations exist within the residuals. Multiple iterations to cull outlier points leaves about 1200 observations fitted for each band. Figure 2 gives the lunar phase function for the ROLO 555 nm band, shown by plotting the model fit residuals as vertical line segments joining the data points and corresponding modeled reflectance. The mean absolute residual for this band  $U_{555}=0.95\%$ ; the mean residual over all bands is similar.

A challenging task is relating the measurement uncertainties to the precision of the resulting model. For each band, there are 9 coefficients determined, plus 8 that are constant across all bands. With about  $N = 1200$  measurement points per band, the fit is highly overdetermined. The data are reasonably uniformly distributed over phase angle, which has the strongest dependence in the model. The residuals show no discernible correlation with any of the model parameters, so the formal assessment would be that the model variation from the true value, apart from a scale factor for each band, is roughly  $\frac{U}{\sqrt{N}}$ , or 0.02% and 0.05% for VNIR and SWIR respectively. A more realistic evaluation comes from scaling (arbitrarily) with the fourth root of  $N$ ; the model precision values become 0.11% and 0.28%.

ROLO model-generated irradiances, calibrated using the star-based procedure described above, exhibit some irregular spectral excursions between bands, while the Moon's reflectance features are known to be broad and shallow.<sup>13,14,16,17</sup> A correction has been developed to adjust the ROLO model results based upon fitting to laboratory reflectance measurements of returned Apollo samples.<sup>18,19</sup> Figure 3 shows the uncorrected ROLO modeled reflectance for  $g=7^\circ$ ,  $\Phi=7^\circ$ ,  $\theta=0$ ,  $\phi=0$ , along with laboratory spectra for two Apollo samples, soil and breccia. A synthesized mixture (95% soil) was scaled  $A' = (a + b\lambda)A$  to fit the ROLO model output while preserving the slope and the depth of the absorption features. The adjustment factors correct each ROLO band to the "Adjusted" curve.

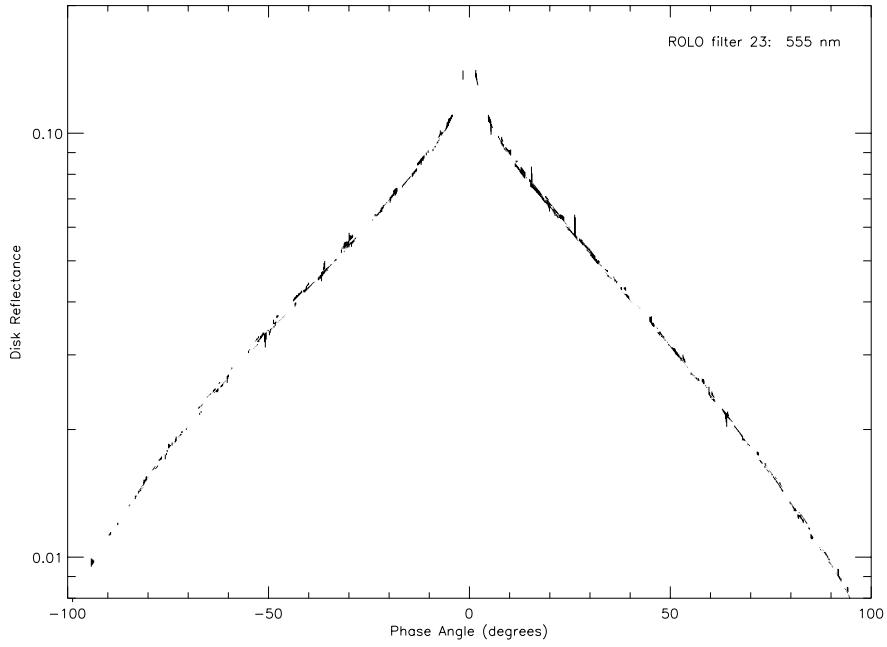


**Figure 2.** Disk Reflectance vs. Phase Angle. The plot symbols are (vertical) lines drawn between the ROLO observational data and the corresponding model results. Indication of the sign of the difference has been lost in the image reproduction.

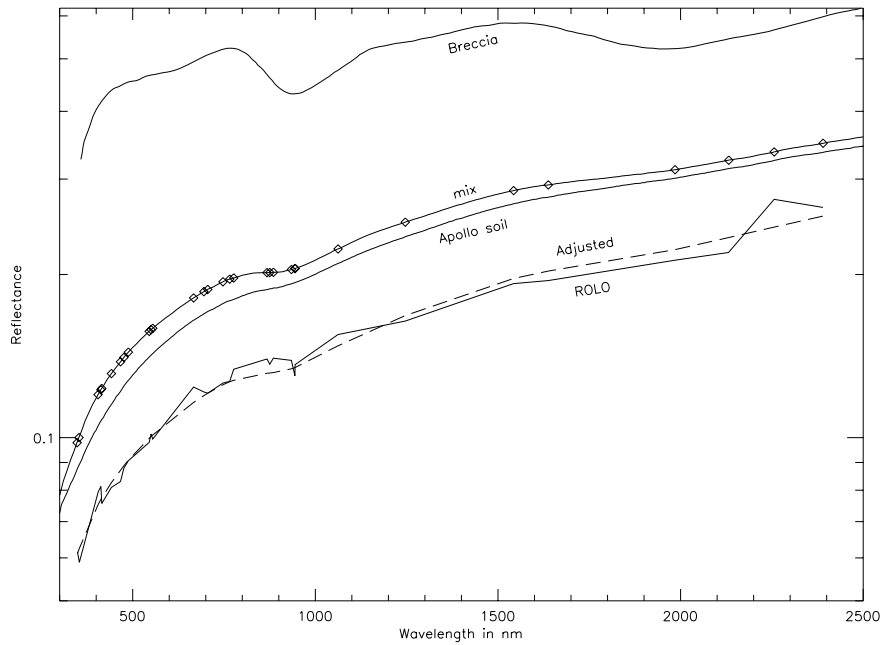


**Figure 3.** Lunar Reflectance Spectra. The diamonds show the ROLO band wavelengths on a 95% soil:breccia mix spectrum, which is scaled to best fit the ROLO model output.

An estimate of the band-to-band radiance calibration uncertainty can be made from the Apollo correction. The correction ranges from  $-11.3\%$  to  $+7.4\%$ , with a standard deviation of  $4.4\%$  and an average absolute value of  $3.5\%$  over all 32 bands. This suggests that the non-statistical relative uncertainty in the radiance scale resulting from our star calibration efforts is about  $4\%$ .

The conversion from irradiance to reflectance, equation 6, specifies a model for the solar spectral irradiance convolved with the RSR functions for the ROLO bands. Solar models currently in common use show differences of several percent in absolute scale, particularly at IR wavelengths. All ROLO work to date has used the 1986 WCRP solar data,<sup>23</sup> and has ignored the  $\sim 0.1\%$  11-year variability in total solar irradiance. Although the computed lunar reflectance has a direct relation to the solar irradiance, differences in solar models will have a second order effect on the ROLO model outputs as long as the same model is used in converting from irradiance to reflectance and back. ROLO is currently undertaking a study to quantify the effects of using different solar models.

#### 4. SPACECRAFT LUNAR IRRADIANCE COMPARISONS

The procedures for spacecraft team interaction with ROLO for lunar calibration have been largely formalized; details are available online at:

**www.moon-cal.org** → Spacecraft Calibration → Information Exchange Items

Calibrations compare ROLO results against spacecraft observations of the Moon processed to disk-equivalent irradiance using the instrument’s nominal calibration. The ROLO model generates the lunar reflectance corresponding to the spacecraft observation geometry, then interpolates to the instrument bands and converts to irradiance. The discrepancy in irradiance (at standard distances) is reported to the instrument team as a percentage difference:

$$P = \left( \frac{I_{\text{inst}}}{I_{\text{ROLO}}} - 1 \right) \times 100\% \quad (8)$$

Complete lunar calibration comparisons have been generated for four instruments<sup>11</sup>: SeaWiFS, EO-1 Hyperion, EO-1 ALI, and the Multi-spectral Thermal Imager (MTI). ROLO image data have supported auxiliary radiometric calibrations for the Japanese Meteorological Agency’s GMS-5 and NOAA GOES-10 geosynchronous weather satellites.<sup>7, 15</sup> Following the 14 April 2003 Terra Deep Space Calibration Maneuver with Lunar View, comparison work is in progress for MODIS, MISR, CERES, and ASTER lunar images.

Example comparison plots of  $P$  (equation 8) are shown in Figure 4 for SeaWiFS, Hyperion, ALI and MTI. The data shown are averages over nearly all of the lunar observations made by each instrument. Details of spacecraft lunar acquisition techniques and development of these comparison are found in Ref. 11. This plot gives an indication of each instrument’s absolute response as measured against the current ROLO irradiance model. Errors in either are indistinguishable in these comparisons; however, systematic error in the ROLO model results would appear as a correlated bias for all instruments.

##### 4.1. Relative Response Trending – SeaWiFS

Long-term instrument response trending with sub-percent precision has been achieved in lunar calibration comparisons with SeaWiFS observations. SeaWiFS has observed the Moon nearly every month since 1997 November. A time-series plot of irradiance comparisons for the first 58 SeaWiFS lunar observations is shown in Figure 5; a band-correlated temporal jitter, attributed to SeaWiFS and probably due to uncertainties in the oversampling factor of the small lunar images, has been averaged and removed from the plotted data. The response trends are quite apparent in bands 7 and 8.

Based on comparisons of the first 66 lunar observations, SeaWiFS has developed an asymptotic time correction for ocean-leaving radiances having the form<sup>2</sup>:

$$\frac{L}{L_0} = a_0 + a_1 t + a_2 e^{-k_1 t} + a_3 e^{-k_2 t} \quad (9)$$

where the  $a$  coefficients are fitted for each band (although not all terms are non-zero for any bands) and the  $k_n$  time constants are  $(200 \text{ day})^{-1}$  and  $(2000 \text{ day})^{-1}$ .



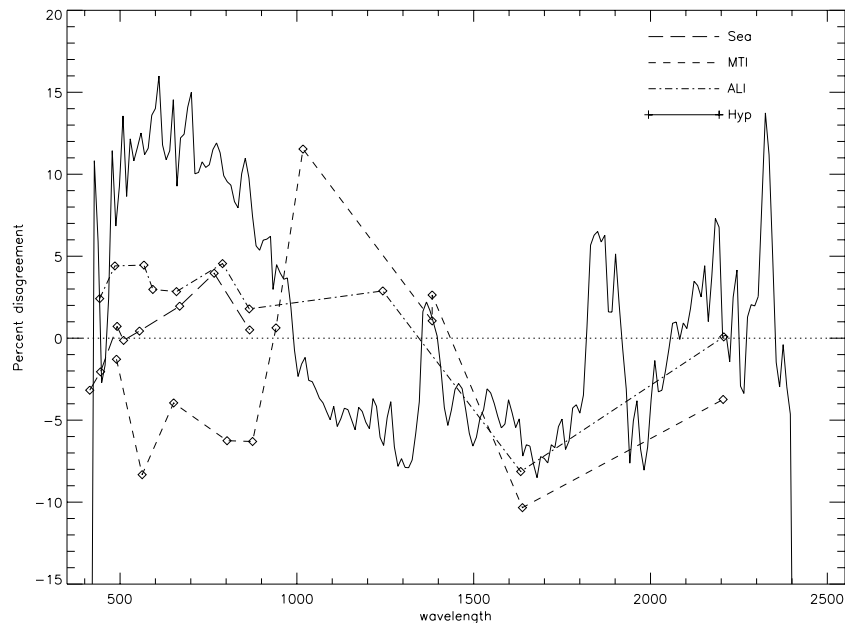


**Figure 4.** Spectral shape of lunar calibration results for four spacecraft instruments. The curve for each instrument is the average of their individual observations. The difference between instruments is largely independent of the lunar model absolute calibration. SeaWiFS is within 4% in all bands, generally rising with wavelength over the first 7 bands; ALI is about 3% high below 1300 nm, and MTI has a wide variation of response, being generally low shortward of 900 nm. Hyperion is about 10% high in the VNIR, 5% low in the SWIR, with rapid spectral variations of several percent. All three instruments with response at 1630 nm are roughly 7% lower than the ROLO model.

The fit residuals of equation 9 range from 0.03% to 0.09% for the eight SeaWiFS bands. This level of precision results from the long time series of lunar observations acquired by SeaWiFS, and to a lesser extent the similarity in phase angles within the series. SeaWiFS observes the Moon fairly consistently near  $7^\circ$  phase, both before and after Full Moon; this represents a compromise to maximize signal strength while avoiding the lunar “opposition effect” — the enhanced backscatter at low phase angles. However, ROLO lunar calibration does not require that all observations be made at similar phase angles.

## 5. SUMMARY

The primary tool for ROLO lunar calibration work is a model of the disk-equivalent lunar irradiance which correctly accounts for the photometric geometries of spacecraft observations of the Moon. This capability derives from a 6+ year set of radiometric observations of the Moon acquired by the project’s ground-based telescopes. The precision currently achieved allows instrument response trending approaching 0.1% per year; however, the absolute scale of the model is still uncertain to several percent. A current major project focus is the assessment of uncertainties in the ROLO irradiance data, particularly the atmospheric extinction correction and development of the absolute calibration and spectral response functions.

Reduction of ROLO at-telescope image data to lunar radiance includes generation of statistics-based pixel value uncertainties. These errors are propagated through the secondary processing routines that yield irradiance data for model fitting. The ROLO lunar reflectance model was developed with the goal of minimizing correlations seen in the fit residuals; the mean absolute residual over all bands is under 1%.

Absolute calibration of the ROLO lunar data and model is derived from observations of the star Vega. The calibration accuracy is dependent upon absolute photon fluxes from astronomical measurements, and also the ROLO atmospheric extinction correction algorithm, which applies to both the lunar images and the calibration observations of Vega. Given the known uncertainties in the ROLO calibration development, the current estimate

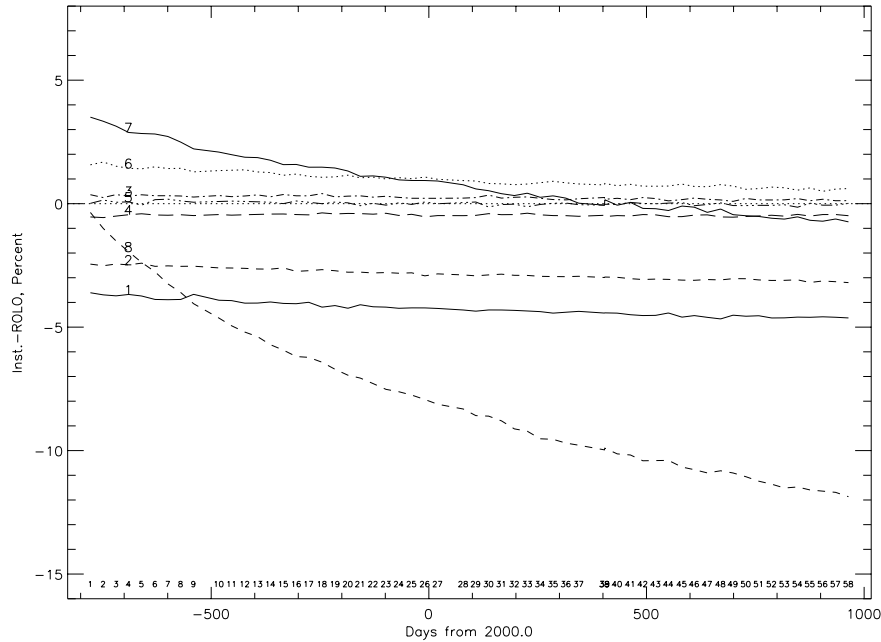


**Figure 5.** SeaWiFS lunar irradiance comparison. Successive lunar observations are indexed along the bottom of the figure.

of accuracy is 5–10% absolute. This is comparable to the scatter in lunar irradiance comparison data from several spacecraft instruments, each utilizing their own calibration pathway. The need to reduce uncertainty in the ROLO absolute scale has driven development of a calibration method that does not involve an exoatmospheric source. A field calibration campaign, in collaboration with NASA, the University of Arizona, and NIST, has measured the ROLO system responsivity using a collimated light source which has a primary calibration from NIST. The collimator system also has been used to measure the relative spectral response for several ROLO bands using the NIST Traveling SIRCUS facility; measurements of most or all bands are planned for future field work.

## ACKNOWLEDGMENTS

The authors thank the calibration teams for SeaWiFS, Hyperion, ALI, and MTI for use of their lunar irradiance measurements in this paper. The ROLO project has been supported by the NASA Office of Earth Science through Goddard Space Flight Center under contracts S-41359-F and NNG04HK38I.

## REFERENCES

1. J. M. Anderson, K. J. Becker, H. H. Kieffer, and D. N. Dodd. Real-time control of the Robotic Lunar Observatory telescope. *Pub. Astronomical Soc. Pacific*, 111:737–749, jun 1999.
2. R. A. Barnes, R. E. Eplee Jr., F. S. Patt, H. H. Kieffer, T. C. Stone, G. Meister, and J. J. Butler C. R. McClain. Comparison of the on-orbit response history of SeaWiFS with the USGS lunar model. *Applied Optics*, accepted for publication:–, 2004.
3. R. A. Barnes, Jr. R. E. Eplee, and F. S. Patt. SeaWiFS measurements of the Moon. *Proc. SPIE*, 3438:311–324, 1998.
4. R. A. Barnes, Jr. R. E. Eplee, F. S. Patt, and C. R. McClain. Changes in the radiometric response of SeaWiFS determined from lunar and solar-based measurements. *Appl. Opt*, 38:4649–4664, 1999.
5. F. Castelli and R. L. Kurucz. Model atmospheres for vega. *Astron. Astrophys.*, 281:817–832, 1994.
6. A. N. Cox. *Allens’ Astrophysical Quantities*. Springer-Verlag, New York, 1999. 719 pp.

7. I. F. Grant, H. H. Kieffer, T. C. Stone, and J. M. Anderson. Lunar calibration of the GMS-5 visible band. In *Proceedings of the International Geophysics and Remote Sensing Symposium 2001*, volume VI, pages 2769–2771, Piscataway, NJ, 2001. IEEE Publications.
8. R. O. Gray. The absolute flux calibration of Strömngren *uvby* photometry. *Astronom. J.*, 116:482–485, 1998.
9. D. S. Hayes. Stellar absolute fluxes and energy distributions from 0.32 to 4.0 microns. In *Calibration of Fundamental Stellar Quantities; Proceedings of IAU Symposium No. 111, Como, Italy, May 24-29, 1984*, pages 225–252, Dordrecht, 1985. D. Reidel Publishing Co.
10. H. H. Kieffer and J. A. Anderson. Use of the Moon for spacecraft calibration over 350–2500 nm. *Proc. SPIE*, 3438:325–335, 1998.
11. H. H. Kieffer, T. C. Stone, R. A. Barnes, S. Bender, R. E. Eplee Jr., J. Mendenhall, and L. Ong. On-orbit radiometric calibration over time and between spacecraft using the Moon. *Proc. SPIE*, 4881:287–298, 2003.
12. H. H. Kieffer and R. L. Wildey. Establishing the Moon as a spectral radiance standard. *J. of Atmospheric and Oceanic Technology*, 13(2):360–375, 1996.
13. A. P. Lane and W. M. Irvine. Monochromatic phase curves and albedos for the lunar disk. *Astron. J.*, 78:267–277, 1973.
14. P. G. Lucey, B. R. Hawke, C. M. Pieters, J. W. Head, and T. B. McCord. A compositional study of the Aristarchus region of the Moon using near-infrared spectroscopy. *J. Geophys. Res.*, 91:D344–D354, 1986.
15. M. S. Maxwell and H. H. Kieffer. Calibrating the GOES imager visible spectral band using the moon as an irradiance standard. *Proc. SPIE*, 3439:136–144, 1998.
16. T. B. McCord, R. N. Clark, B. R. Hawke, L. A. McFadden, P. D. Owensby, and C. M. Pieters. Moon - near-infrared spectral reflectance, a first good look. *J. Geophys. Res.*, 86:10883–10892, Nov. 10 1981.
17. T. B. McCord and T. V. Johnson. Lunar spectral reflectivity (.3 to 2.5 microns) and implications for remote mineralogical analysis. *Science*, 169:854–858, 1970.
18. C. M. Pieters. The Moon as a spectral calibration standard enabled by lunar samples: The clementine example. In *Workshop on New Views of the Moon II: Understanding the Moon Through the Integration of Diverse Datasets. Flagstaff, AZ. Lunar and Planetary Instit. Contrib.*, pages 47–48, September 1999.
19. C. M. Pieters and J. F. Mustard. Exploration of crustal/mantle material for the earth and Moon using reflectance spectroscopy. *Rem. Sens. Environ.*, 24:151–178, 1988.
20. T. C. Stone and H. H. Kieffer. Absolute irradiance of the Moon for on-orbit calibration. *Proc. SPIE*, 4814:211–221, 2002.
21. T. C. Stone, H. H. Kieffer, and J. M. Anderson. Status of use of lunar irradiance for on-orbit calibration. *Proc. SPIE*, 4483:165–175, 2002.
22. D. W. Strecker, E. F. Erickson, and F. C. Witteborn. Airborne stellar spectrometry from 1.2 to 5.5 microns - absolute calibration and spectra of stars earlier than M3. *Astrophys. J. Supp.*, 41:501–512, 1979.
23. C. Wehrli. Spectral solar irradiance data. World Climate Research Program (WCRP) Publication Series No. 7, WMO ITD-No. 149, 1986. pp. 119-126.